Available online at www.sciencedirect.com
SCIENCE DIRECT®
C. R. Chimie 6 (2003) 343–352
COMPTES RENDUS CHIMIE

Full paper/Mémoire

Photomagnetism in $C_xCo_4[Fe(CN)_6]_{(8+x)/3}\cdot n\ H_2O$ Prussian blue analogues: looking for the maximum photo-efficiency

Anne Bleuzen [a,*], Virginie Escax [a], Jean-Paul Itié [b], Pascal Münsch [b], Michel Verdaguer [a]

[a] *Laboratoire de chimie inorganique et matériaux moléculaires, unité CNRS 7071, université Pierre-et-Marie-Curie, Bât. F 74, 4, place Jussieu, 75252 Paris cedex 05, France*
[b] *Laboratoire pour 1'utilisation du rayonnement électromagnétique, UMR CNRS 130–CEA–MENRS, Bât. 209d, université Paris-Sud, BP34, 91898 Orsay cedex, France*

Received 30 October 2002; accepted 29 January 2003

Abstract

A family of CoFe Prussian blue analogues $C_xCo_4[Fe(CN)_6]_{(8+x/3)}\square_{(4-x)3}$ (x = amount of alkali cation inserted per conventional cell, C = Na, K, Rb, Cs; □ = $[Fe(CN)_6]$ vacancy) have been synthesized and characterized. Their photomagnetic properties have been investigated by magnetic measurements before and after irradiation and X-ray diffraction under continuous irradiation. We show that the photo-induced magnetism depends on several parameters: (*i*) the amount of Co^{III}–Fe^{II} diamagnetic excitable pairs per cell; (*ii*) the amount of $[Fe(CN)_6]$ vacancies, and (*iii*) the amount and nature of the alkali cations per cell. We evidence a discontinuity in the properties' change when the amount of alkali cation x varies, around $x = 1$. For $x < 1$, there is an excitation of diluted Co^{III}–Fe^{II} diamagnetic pairs in a phase mainly composed of magnetic Co^{II}–Fe^{III} entities within the same structural phase through a second-order continuous transformation. For $x \geq 1$, the formation of domains mainly composed of Co^{II}–Fe^{III}* metastable magnetic pairs in a phase mainly composed of Co^{III}–Fe^{II} diamagnetic ones through a first-order discontinuous transition is observed. The study points out that sodium derivatives are more efficient than the others. Among them, $Na_1Co_4[Fe(CN)_6]_3\square_1$ is predicted to be the most efficient one. ***To cite this article: A. Bleuzen et al., C. R. Chimie 6 (2003)***.

Résumé

Une famille de composés analogues du bleu de Prusse $C_xCo_4[Fe(CN)_6]_{(8+x)/3}\square_{(4-x)\ 3}$ (x = quantité de cation alcalin inséré par maille conventionnelle C = Na, K, Rb, Cs ; □ = lacune de $[Fe(CN)_6]$) a été synthétisée et caractérisée. Les propriétés photomagnétiques ont été étudiées par des mesures de magnétisme avant et après irradiation et par diffraction des rayons X sous irradiation continue. Nous montrons que l'effet photo-magnétique dépend de plusieurs paramètres : (*i*) nombre de paires diamagnétiques Co^{III}–Fe^{II} photoexcitables par maille ; (*ii*) nombre de lacunes de $[Fe(CN)_6]$ et (*iii*) nature et nombre de cation alcalin inséré par maille. Nous mettons en évidence une discontinuité dans l'évolution des propriétés quand le nombre x de cations alcalins insérés prend des valeurs proches de $x = 1$. Pour $x < 1$ il y a excitation de paires Co^{III}–Fe^{II} diluées au sein d'une phase majoritairement composée de paires magnétiques Co^{II}–Fe^{III} via une transformation du second ordre continue. Pour $x \geq 1$,

* Corresponding author.
E-mail address: bleuzen@ccr.jussieu.fr (A. Bleuzen).

DOI: 10.1016/S1631-0748(03)00043-2

on observe la formation photo-induite de domaines majoritairement composés de paires Co^{II}–Fe^{III}* excitées magnétiques dans une phase majoritairement composée de paires diamagnétiques Co^{III}–Fe^{II} via une transition du premier ordre discontinue ($x \geq 1$). L'étude montre que les dérivés du sodium sont les plus efficaces. Nous prévoyons que parmi ces composés, $Na_1Co_4[Fe(CN)_6]_3\square_1$ est le plus efficace. ***Pour citer cet article : A. Bleuzen et al, C. R. Chimie 6 (2003)***.

Keywords: Prussian blue analogues; photomagnetism; electron transfer; X-ray diffraction

Mots clés : analogues du bleu de Prusse ; photomagnétisme ; transfert d'électron ; diffraction des rayons X

1. Introduction

The interest for photomagnetic molecular materials is growing. A compound is called photomagnetic when its magnetic properties are modified by light. The recent development of this research field is partly due to the potential applications of such systems to information storage: optical devices are expected to allow high density of information.

Recently, an increasing number of photomagnetic molecular materials have been synthesized, showing spectacular effects and involving various and complex mechanisms [1–9]. Among them are CoFe Prussian blue analogues. Hashimoto and co-workers discovered their photomagnetic properties in 1996 in the compound $K_{0.2}Co_{1.4}[Fe(CN)_6]_1 \cdot 6.9\,H_2O$ [10]. This was the first three-dimensional compound in which a metal-metal photo-induced electron transfer Co^{III}–$Fe^{II} \rightarrow Co^{II}$–$Fe^{III}$*, leading to the formation of excited metastable magnetic pairs of long lifetime at low temperature [10, 11], is responsible for the photomagnetic properties. We showed in a previous work that a bond lengthening of the cobalt-ligand bonds accompanies the photo-induced electron transfer [12]. This system is one of the most studied [13–21] and we undertook a systematic study in order to identify the parameters responsible for the photomagnetism [12, 22–26].

The face-centred cubic $Co_4[Fe(CN)_6]_{8/3}\square_{4/3} \cdot n\,H_2O$ Prussian blue presents intrinsic $[Fe(CN)_6]$ vacancies $\square$ due to the stoichiometry. The insertion of alkaline cations in the structure is accompanied by the filling of the vacancies by the anionic ferricyanide to ensure electroneutrality of the solid, according to:

$$Co_4[Fe(CN)_6]_{8/3}\square_{4/3} \cdot n\,H_2O + xC^+ + x/3[Fe(CN)_6] \rightarrow C_xCo_4[Fe(CN)_6]_y\square_{4-y} \cdot n'\,H_2O$$

with $y = (8 + x)/3$.

The chemical formulae, above and below, are given for one conventional unit cell.

In the present paper, we study the photomagnetic properties of the CoFe Prussian blue analogues $C_xCo_4[Fe(CN)_6]_{(8+x)/3}\square_{(4-x)/3}$ where C = Cs, Rb, K and Na.

2. Experimental section

2.1. Samples

Potassium hexacyanoferrate(III) (Acros, puriss. p.a.), cobalt(II) nitrate (Acros, p.a.) and cesium (Aldrich, puriss. p.a.), rubidium (Aldrich, p.a.), potassium (Acros, p.a.) and sodium (Acros, p.a.) nitrates were used as received.

Synthesis conditions were adapted to the nature of the alkali cation. We observed that the affinity of the alkali cation for the inorganic network increases with increasing size. For this reason, the rubidium derivatives were prepared with diluted aqueous solutions, while potassium and sodium ones were synthesized using concentrated aqueous solutions.

The cesium derivatives were synthesized as previously described [25]. The rubidium derivatives were prepared using diluted solutions, by addition of a solution made of cobalt(II) nitrate and various amount of rubidium nitrate to a potassium hexacyanoferrate(III) solution. To obtain the potassium and sodium derivatives, the cobalt(II) nitrate solution was added to a concentrated solution made of potassium hexacyanoferrate(III) and various amounts of alkali cations salt always used in large excess.

In all the syntheses, the initial pH of the solutions was adjusted to 5 using HNO_3 diluted solutions. The addition rate was regulated to last 3 h. The powders were centrifuged, washed three times with distilled water and allowed to dry in air.

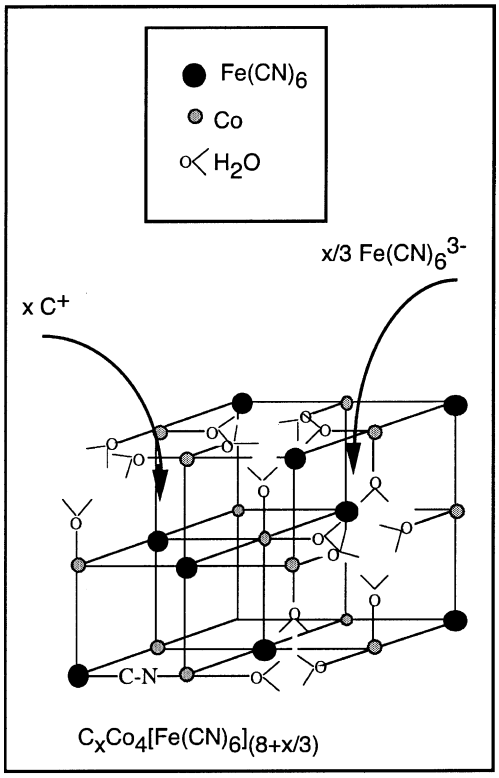

Fig. 1. Schematic conventional face-centred cubic cell of a Prussian blue analogue.

The X-ray powder diffraction patterns of all the compounds are consistent with a cubic system, face-centred network, schematised in Fig. 1.

The element analyses, related to the chemical formulae for an fcc conventional cell $C_xCo_4[Fe(CN)_6]_{(8+x)/3}\square_{(4-x)/3}$ are reported in Table 1. In the following, the compounds are named C_x, indicating the nature of the alkali cation C in the compound and its x amount per cell. The chemical formulae of compounds **Cs$_{0.3}$**, **Cs$_{0.7}$**, **Cs$_{1.2}$**, and compounds ***C*$_0$** and **Rb$_{1.8}$** given in reference [25] and in reference [24] are also reported. Taking into account the uncertainty in the stoichiometric coefficients (±0.1), all the formulae correspond to neutral samples. The insertion of x alkali cations (C^+) is accompanied by the insertion of $x/3$ additional $[Fe(CN)_6]^{3-}$ anionic entities (Fig. 1).

The oxidation states of the metallic cations at 20 K were quantitatively determined by X-ray absorption near edge spectroscopy (XANES) at the cobalt and iron K edges as previously described [25]. The edge spectra of the compounds containing a mixture of Co^{III} and Co^{II} ions were fairly well reproduced by linear combinations of spectra of two model samples **Rb$_{1.8}$** and ***C*$_0$**, respectively composed of a majority of Co^{III}–Fe^{II} and Co^{II}–Fe^{III} pairs at 20 K [27]. Knowing the percentage of Co^{II} and Co^{III} ions in the models [25, 27], the percentage of Co^{III} ions in each compound was obtained (Table 2).

2.2. Instrumentation

Photomagnetic experiments were carried out with a Quantum Design MPMS-5S magnetometer working in the dc mode, equipped with a multi-wire silica optical fibre. The fibre was connected to a broadband source of light (tungsten halogen lamp, 100 W), through interferential filters (100-nm bandwidth). A cut-off filter provided a high intensity in the 750 ± 50 nm range. The power received by the irradiated sample is estimated to P = 60 mW cm^{-2}. The measurements were performed over the 10–300-K temperature range with an applied magnetic field of 500 G. In a first step, 3 mg of powder (pellet-shaped) was slowly cooled from 300 to 10 K to avoid quenching phenomena and then irradiated at 10 K during 4 h. The magnetic field was applied as soon as the irradiation began.

The temperature was raised above the Curie temperature and decreased again before measurement to get the Field Cooled Magnetisation (FCM) curve over the 10–300 K temperature range. The temperature was then raised above T = 200 K. At that temperature, all the samples relaxed and came back to their initial ground state, which allows us to measure then the magnetisation before irradiation ($M_{initial}$) over the 10–300-K temperature range. To compare the samples, the amount of compound and the procedure were exactly the same. Excepted for the sodium derivatives, we checked that the wavelength range used for irradiation was the most efficient one.

Energy-dispersive X-ray diffraction patterns were recorded at 10 K over the 0.5–70 keV energy range on the DW11A energy-dispersive X-ray beam of the DCI ring of the LURE synchrotron facility at Orsay, France. The orientation of the detector was fixed at Θ = 5.8457° for compound **Cs$_{0.7}$** and Θ = 4.003° for compound **Na$_{1.8}$**. The orientation was checked by measuring the X-ray pattern of a copper foil at room temperature. For the measurements, the powders were spread on between two tapes and slowly cooled from 300 to 10 K. At low temperature, the white X-ray beam

Table 1
Names, element analysis and proposed formulae for all compounds.

Sample/Element	***C***	**Co**	**Fe**	C	N	H	O
$\mathbf{C_0}$				$K_{0.1}Co_4[Fe(CN)_6]_{2.7}\square_{1.3}\cdot 19\ H_2O$			
$\mathbf{Cs_{0.3}}$				$Cs_{0.3}Co_4[Fe(CN)_6]_{2.8}\square_{1.2}\cdot 18\ H_2O$			
$\mathbf{Cs_{0.45}}$	*Cs*	proposed formula: $Cs_{0.45}Co_4[Fe(CN)_6]_{2.8}\square_{1.2}\cdot 18\ H_2O$					
% exp.	5.10	20.40	13.65	16.97	19.21	3.11	21.51
(% calc.)	(4.93)	(19.43)	(12.89)	(16.63)	(19.39)	(2.99)	(23.74)
$\mathbf{Cs_{0.7}}$				$Cs_{0.7}Co_4[Fe(CN)_6]_{2.9}\square_{1.1}\cdot 16\ H_2O$			
$\mathbf{Cs_{0.95}}$	*Cs*	proposed formula: $Cs_{0.95}Co_4[Fe(CN)_6]_{3.0}\square_{1.0}\cdot 16\ H_2O$					
% exp.	9.90	18.41	12.85	16.34	18.47	2.25	21.77
(% calc.)	(9.82)	(18.33)	(13.03)	(16.81)	(19.60)	(2.51)	(19.90)
$\mathbf{Cs_{1.2}}$				$Cs_{1.2}Co_4[Fe(CN)_6]_{3.2}\square_{0.8}\cdot 16\ H_2O$			
$\mathbf{Cs_2}$	*Cs*	proposed formula: $Cs_{2.0}Co_4[Fe(CN)_6]_{3.3}\square_{0.7}\cdot 13\ H_2O$					
% exp.	17.35	15.17	12.09	16.87	18.91	1.13	18.48
(% calc.)	(18.52)	(16.43)	(12.84)	(16.07)	(19.32)	(1.82)	(14.49)
$\mathbf{Rb_{0.6}}$	*Rb*	proposed formula: $Rb_{0.6}Co_4[Fe(CN)_6]_{2.9}\square_{1.1}\cdot 20\ H_2O$					
% exp.	3.81	16.78	11.86	17.94	19.13	2.40	28.08
(% calc.)	(4.06)	(18.68)	(12.83)	(16.56)	(19.31)	(3.19)	(25.35)
$\mathbf{Rb_{1.3}}$	*Rb*	proposed formula: $Rb_{1.3}Co_4[Fe(CN)_6]_{3.1}\square_{0.9}\cdot 14\ H_2O$					
% exp.	8.56	17.81	13.34	16.77	19.35	2.05	22.12
(% calc.)	(8.85)	(18.77)	(13.78)	(17.79)	(20.74)	(2.25)	(17.83)
$\mathbf{Rb_{1.8}}$				$Rb_{1.8}Co_4[Fe(CN)_6]_{3.3}\square_{0.7}\cdot 13\ H_2O$			
$\mathbf{K_{0.85}}$	*K*	proposed formula: $K_{0.85}Co_4[Fe(CN)_6]_{2.95}\square_{1.05}\cdot 18\ H_2O$					
% exp.	2.47	17.61	12.76	18.58	21.18	2.51	24.89
(% calc.)	(2.55)	(19.35)	(13.52)	(17.45)	(20.35)	(2.98)	(23.63)
$\mathbf{K_{1.8}}$	*K*	proposed formula: $K_{1.8}Co_4[Fe(CN)_6]_{3.3}\square_{0.7}\cdot 14\ H_2O$					
% exp.	5.46	18.76	13.86	18.36	20.53	2.34	20.69
(% calc.)	(5.59)	(18.74)	(14.65)	(16.84)	(22.05)	(2.24)	(17.81)
$\mathbf{Na_{1.3}}$	*Na*	proposed formula: $Na_{1.3}Co_4[Fe(CN)_6]_{3.1}\square_{0.9}\cdot 14\ H_2O$					
% exp.	2.47	19.54	13.82	18.94	21.62	2.35	21.26
(% calc.)	(2.54)	(20.06)	(14.73)	(19.01)	(22.17)	(2.40)	(19.06)
$\mathbf{Na_{1.8}}$	*Na*	proposed formula: $Na_{1.8}Co_4[Fe(CN)_6]_{3.3}\square_{0.7}\cdot 14\ H_2O$					
% exp.	3.02	18.55	14.60	19.06	21.54	2.19	20.04
(% calc.)	(3.37)	(19.18)	(14.98)	(19.35)	(22.56)	(2.29)	(18.23)

induces the $Co^{III}(LS)$–$Fe^{II}(LS) \rightarrow Co^{II}(HS)$–$Fe^{III}(LS)$ photo-induced electron transfer. The X-ray source being the probe beam as well as the pumping beam makes sure that the whole diffracting sample is irradiated.

The study of the photo-excitation process was carried out at 10 K under continuous irradiation. X-ray powder diffraction patterns were recorded for increasing irradiation times (Figs. 2 and 3). For the first point, the acquisition time was 15 s. For subsequent points, the acquisition time was 30 s. During this time interval, the pattern change can be neglected. For clarity, the diffractograms in Figs. 2 and 3 are presented in the energy range containing the two most intense reflections.

3. Results and discussion

In order to identify the parameters of the system responsible for the photomagnetism, we first studied the photomagnetic properties of a series of $Cs_xCo_4[Fe(CN)_6]_{(8+x)/3}\square_{(4-x)/3}$ compounds in which we varied the amount of cesium cations. In a second step, we studied the photomagnetic properties of other alkali derivatives, $C_xCo_4[Fe(CN)_6]_{(8+x)/3}\square_{(4-x)/3}$,

Table 2
Percentage of Co^{III} at 20 K, from linear combination of the X-ray absorption spectra of the model compounds $\mathbf{Rb_{1.8}}$ and $\mathbf{C_0}$.

Sample	% Co^{III} at 20 K
$\mathbf{C_0}$	0
$\mathbf{Cs_{0.3}}$	7
$\mathbf{Cs_{0.45}}$	14
$\mathbf{Cs_{0.7}}$	40
$\mathbf{Cs_{0.95}}$	63
$\mathbf{Cs_{1.2}}$	66
$\mathbf{Cs_2}$	82
$\mathbf{Rb_{0.6}}$	37
$\mathbf{Rb_{1.3}}$	58
$\mathbf{Rb_{1.8}}$	82
$\mathbf{K_{0.85}}$	62
$\mathbf{K_{1.8}}$	66
$\mathbf{Na_{1.3}}$	78
$\mathbf{Na_{1.8}}$	78

varying the nature of the alkali cation (C = Rb, K, Na), which were then compared to those of the first series.

3.1. Photomagnetism of the cesium derivatives

The photomagnetic properties of cesium derivatives were already discussed in a previous paper [25]. We showed that the photomagnetic effect depends on a compromise between the number of Co^{III}–Fe^{II} diamagnetic pairs and the network flexibility. Since then, the series has been completed and enables us to go further in the conclusions.

The magnetisation curves of compounds $\mathbf{Cs_{0.3}}$–$\mathbf{Cs_{0.7}}$ before and after irradiation over the 10–30-K temperature range are presented in Fig. 4. These compounds contain less than one alkali cation per cell. The corresponding magnetisation curves for compounds $\mathbf{Cs_{0.95}}$–$\mathbf{Cs_2}$, with one alkali cation per cell or more, are given in Fig. 5. The change in the photomagnetic properties along the series of caesium derivatives is discontinuous. The discontinuity appears around $x = 1$.

Before irradiation, $\mathbf{Cs_{0.3}}$ is already ferrimagnetic, with a Curie temperature T_C = 17 K [25] (Fig. 4), in agreement with the weak amount of diamagnetic pairs at 20 K (Table 2). After irradiation, the magnetisation at 10 K and T_C slightly increase which means that the number of magnetic neighbours increases in the ferrimagnetic phase after irradiation. Co^{III}–Fe^{II} isolated diamagnetic pairs are photo-transformed into metastable (Co^{II}–Fe^{III})* magnetic ones.

As the amount of cesium increases in the compounds [$\mathbf{Cs_{0.45}}$–$\mathbf{Cs_{0.7}}$], the initial magnetization at 10 K decreases. The Curie temperature also decreases, which means that the number of paramagnetic neighbours is decreasing in the sample. However, the magnetisation and the Curie temperature after irradiation at 10 K are approximately the same in the three compounds, close to the ones of the alkali cation free sample. Co^{III}–Fe^{II} isolated diamagnetic pairs are nearly all photo-transformed into metastable (Co^{II}–Fe^{III})* magnetic ones. The determining factor of photomagnetism is the number of diamagnetic pairs present at low temperature before irradiation.

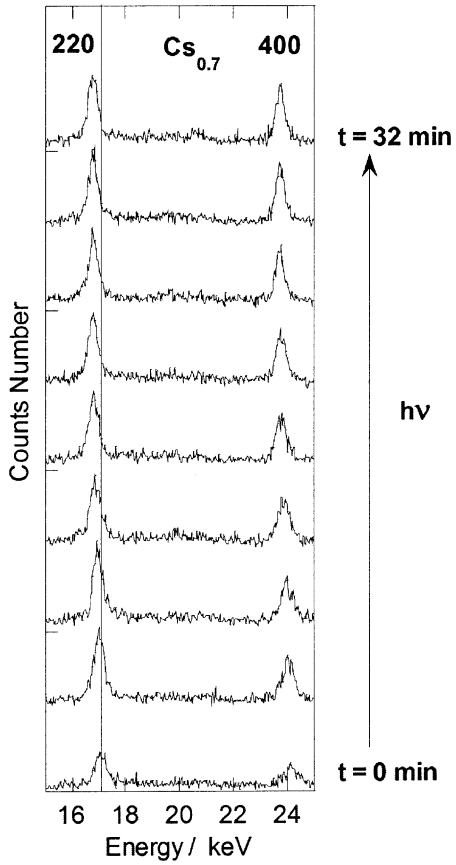

Fig. 2. Energy-dispersive X-ray diffraction patterns recorded at 10 K for increasing irradiation time in compound $\mathbf{Cs_{0.7}}$ (220 and 400 reflections).

$\mathbf{Cs_{0.95}}$ is weakly paramagnetic before irradiation (Fig. 5) in agreement with the important amount of Co^{III}–Fe^{II} diamagnetic pairs at low temperature before irradiation (Table 2). After irradiation, the compound becomes ferrimagnetic below a Curie temperature slightly above the ones of the previous compounds

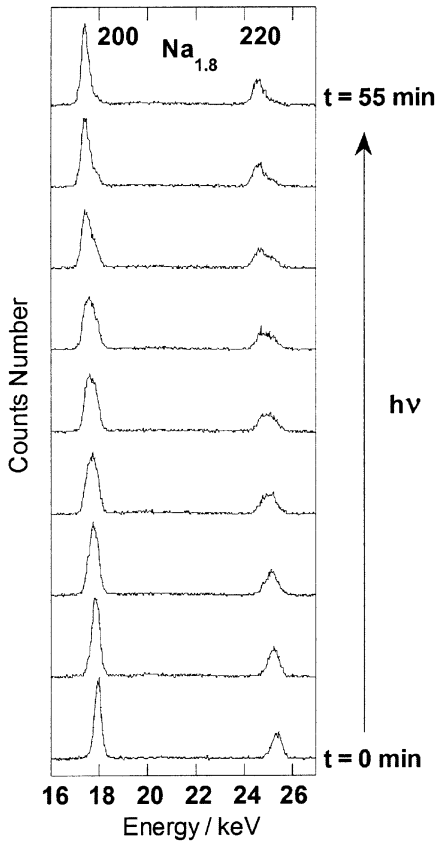

Fig. 3. Energy-dispersive X-ray diffraction patterns recorded at 10 K for increasing irradiation time in compound **$Na_{1.8}$** (200 and 220 reflections).

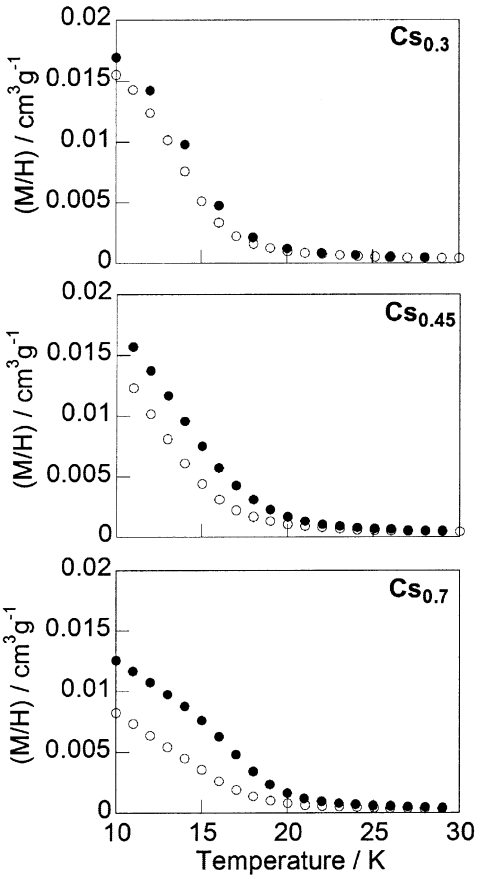

Fig. 4. Thermal variation of the reduced magnetisation (M/H) per gram of compounds **$Cs_{0.3}$**, **$Cs_{0.45}$** and **$Cs_{0.7}$** over the 10–30-K temperature range before (□) and after (•) irradiation.

(**$Cs_{0.3}$**–**$Cs_{0.7}$**), but the magnetisation at 10 K is far less than the magnetisation at 10 K in the three previous compounds. The Curie temperature being proportional to the amount of magnetic neighbours, its value in irradiated **$Cs_{0.95}$** shows that the photo-induced ferrimagnetic phase is mainly composed of Co^{II}–Fe^{III}* metastable pairs and not of Co^{II}–Fe^{III}* pairs diluted in Co^{III}–Fe^{II} diamagnetic ones, which would lead to a lower Curie temperature. The magnetisation at 10 K far less than in the previous compounds indicates that only limited domains of diamagnetic Co^{III}–Fe^{II} pairs are photo-transformed into limited domains of metastable (Co^{II}–Fe^{III})* magnetic pairs. When the amount of alkali cations increases (**$Cs_{1.2}$**–**Cs_2**), the magnetisation curve before irradiation is approximately the same for these two compounds in agreement with a same amount of diamagnetic pairs at low temperature (Table 2). Only the magnetisation curves after irradiation varies. As the amount of alkali cation increases, the magnetisation at 10 K after irradiation progressively decreases accompanied by a progressive loss of the magnetic order. However, the Curie temperature of the ferrimagnetic contribution remains close to the one of all the other compounds which indicates again the formation of domains mainly composed of Co^{II}–Fe^{III}* pairs. The small magnetisation value at 10 K is due to the limited number and/or size of the photo-induced Co^{II}–Fe^{III}* domains. We ascribe the loss of photomagnetic properties to the rigidity of the inorganic network. The rigidity prevents the lengthening of the cobalt–ligand bonds (about 0.15 Å) accompanying the photo-induced electron transfer from Co(III)(low spin)–Fe(II)(low spin) to Co(II)(high spin)–Fe(III)(low spin) and the single occupancy of the two antibonding e_g* orbitals of cobalt(II) [12, 25]. The

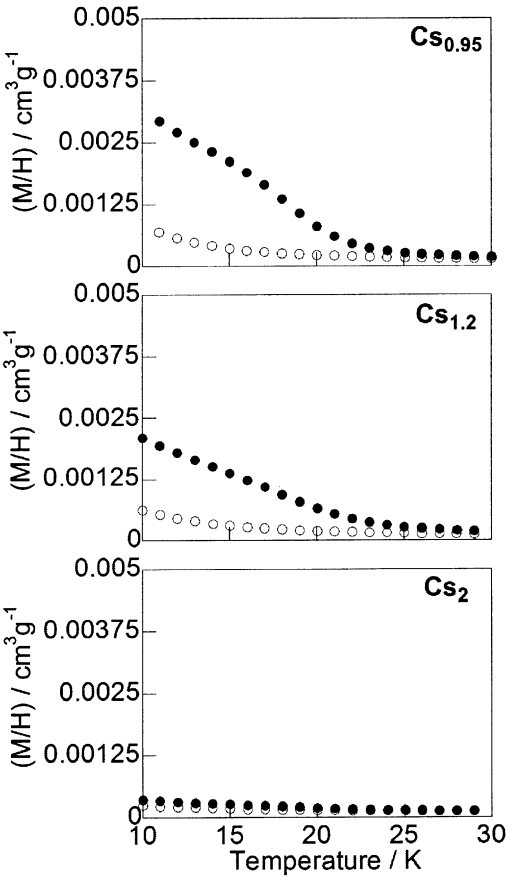

Fig. 5. Thermal variation of the reduced magnetisation (M/H) per gram of compounds **$Cs_{0.95}$**, **$Cs_{1.2}$** and **Cs_2** over the 10–30-K temperature range before (○) and after (•) irradiation.

increase of the rigidity of the network is related to the increasing number of $[Fe(CN)_6]$ filling the vacancies when the amount of alkali cations increases. It may also be related to the number and to the size of cesium cations since their interactions with the $Co_4[Fe(CN)_6]_{(8+x)/3}$ network may rigidify the structure. To summarize, for the compounds containing more than one alkali cation per cell, domains of diamagnetic Co^{III}–Fe^{II} pairs are photo-transformed into domains of metastable $(Co^{II}–Fe^{III})^*$ magnetic entities. Photomagnetism is limited by the network flexibility.

The study evidences a discontinuity of the photomagnetic properties around $x = 1$. This discontinuity around $x = 1$ is not specific to the photomagnetic properties of the compounds. It also appears in the number of diamagnetic pairs per cell for example. When $x < 1$, the amount of diamagnetic pairs per cell is proportional to the number of alkali cation per cell. It is no more the case for $x \geq 1$ (Table 2). The stoichiometry $C_1Co_4[Fe(CN)_6]_3\square_1$ ($x = 1$) is very particular. For this stoichiometry, the number of alkali cation and the number of $[Fe(CN)_6]$ vacancies per cell are exactly the same. For $x < 1$, the alkali cations are diluted, whereas the vacancies are concentrated in the compounds. The flexibility is important so that the determining factor is the number of diamagnetic pairs. For $x > 1$, on the contrary, the alkali cations are now concentrated, whereas the vacancies are diluted in the compounds and the determining factor becomes the network flexibility.

3.2. Photomagnetism of other alkali cations derivatives

To compare the photomagnetic properties of cesium and other alkali cations derivatives, it is necessary (i) to get $C_xCo_4[Fe(CN)_6]_{(8+x)/3}$ compounds with exactly the same amount x of different alkali cations C and (ii) to quantitatively determine the amount of photo-transformed pairs. In order to compare the photomagnetic properties of the compounds, we define the photomagnetic efficiency E as $(M_{final} - M_{initial})/M_{initial}$ ($M_{initial}$ and M_{final} are the magnetisations at 10 K before and after irradiation respectively). This so-defined E evidently involves a part related to the pure photo-excitation effect, i.e. the creation of magnetic pairs and a part related to the magnetic response of the sample to the external field. In magnetically ordered phase, the magnetic response depends on the applied magnetic field in a non-linear way. In the present study, we propose to use E to compare, in the same experimental conditions, the photomagnetic response of compounds $C_xCo_4[Fe(CN)_6]_{(8+x)/3}$. For a given value of x, only the nature of C varies. If the photomagnetic properties do not depend on the nature of C, very close values of E are expected. On the contrary, if the photomagnetic properties depend on the nature of C, different value of E will arise. The photomagnetic efficiency E is reported in Fig. 6 versus the amount of alkali cations per cell for all the compounds.

When the amount of alkali cation per cell is less than one ($x < 1$), E increases with the amount of alkali cations, independently of the alkali cation nature. As along the caesium derivatives series, the amount of Co^{III}–Fe^{II} diamagnetic pairs increases with the amount of alkali cations per cell. For close values of x, the

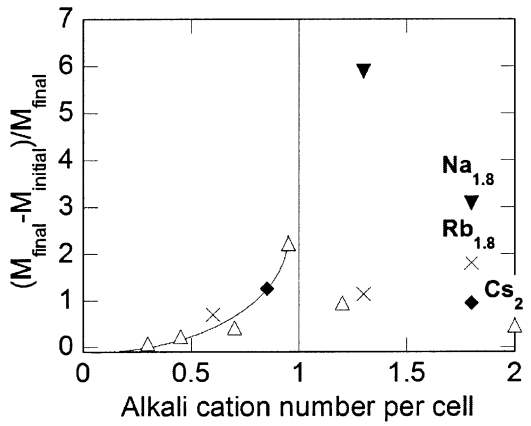

Fig. 6. Photo-efficiency $E = (M_{final} - M_{initial})/M_{initial}$, at 10 K of the Cs (Δ), Rb (×), K(◇) and Na (▼) derivatives vs alkali-cation content per unit cell.

number of diamagnetic pairs at 20 K before irradiation is also close and independent on the nature of the alkali cation (Table 2). The Co^{III}–Fe^{II} isolated diamagnetic pairs are photo-transformed into metastable (Co^{II}–Fe^{III})* magnetic ones. The inorganic network contains a large number of [$Fe(CN)_6$] vacancies (> 1 per cell) and few alkali cations (< 1 per cell). It is flexible enough to allow the photo-transformation of nearly all the diamagnetic pairs. Like in the case of the caesium derivatives, the photomagnetism is a compromise between the number of diamagnetic pairs and the network flexibility. The determining factor is the number of diamagnetic pairs existing at low temperature before irradiation.

When the amount of alkali cations per cell is larger than one ($x \geq 1$), E presents a much more complex variation, not only with the amount, but also with the nature of the alkali cation. This behaviour underlines that numerous parameters are involved in the photomagnetic properties. For a same alkali cation, E decreases with the cation insertion rate x, as in the caesium derivatives series. The decrease is due to the structural flexibility loss. It is noticeable that the ratios E of the compounds $\mathbf{Na_{1.8}}$, $\mathbf{Rb_{1.8}}$ and $\mathbf{Cs_2}$, which contain the same amount of diamagnetic pairs at low temperature before irradiation and have very close stoichiometries (i.e., the same amount of [$Fe(CN)_6$] vacancies and the same average cobalt ion coordination sphere), are very different: E decreases when the size of the alkali cation increases. The result emphasizes the role of the alkali cation on the network flexibility for a constant number of the [$Fe(CN)_6$] vacancies. To be brief, the bigger the cation is, the less flexible the structure is.

3.3. Structural transformation of the $Cs_{0.7}$ and $Na_{1.8}$ derivatives under irradiation

To go further in the understanding of the photo-excitation process, two compounds were selected for X-ray diffraction under continuous irradiation at 10 K: $\mathbf{Cs_{0.7}}$ with $x < 1$ contains a rather high amount of diamagnetic pairs at low temperature, whereas $\mathbf{Na_{1.8}}$ with $x > 1$ still presents enough network flexibility. The diffraction patterns are shown for increasing irradiation times in Fig. 2 for $\mathbf{Cs_{0.7}}$ and in Fig. 3 for $\mathbf{Na_{1.8}}$.

At 10 K, at the very beginning of irradiation, the patterns of both compounds are characteristic of a unique fcc phase.

For $\mathbf{Cs_{0.7}}$, during the excitation process, only one peak appears for each reflection. When the irradiation time increases, the peaks are shifted towards lower energy. After fitting the peaks to a Gaussian line shape, it is possible to conclude that there is no significant line width or intensity change. If two phases with different cell parameters were existing, the line would be broadened. The cell parameter increases. The behaviour is characteristic of a continuous second order transformation within the same phase. Co^{III}–Fe^{II} diamagnetic pairs with short Co– ligand bonds are locally photo-transformed into (Co^{II}–Fe^{III})* pairs with long Co–ligand bonds within the same crystallographic phase. This structural observation is in agreement with the conclusions of the photomagnetic study. The initially ferrimagnetic phase remains ferrimagnetic, only a few randomly distributed Co^{III}–Fe^{II} diamagnetic pairs with short Co to ligand bonds are locally photo-transformed into (Co^{II}–Fe^{III})* magnetic ones through a second-order transformation.

Instead, for $\mathbf{Na_{1.8}}$, after 10 min of irradiation, each reflection on the diffraction pattern splits into two peaks. A new peak appears at lower energy, the intensity of which increases with the irradiation time. The changes indicate the appearance and the growth of a new fcc phase with a longer cell parameter. Domains of Co^{III}–Fe^{II} pairs with short Co-ligand bonds are photo-transformed into domains of metastable Co^{II}– Fe^{III}* pairs with long cobalt-ligand bonds. This behaviour is characteristic of a first-order transition, in agreement with the conclusions of the photomagnetic study: lim-

ited diamagnetic domains mainly composed of Co^{III}–Fe^{II} pairs (with a short cell parameter) are photo-transformed into ferrimagnetic ones, mainly composed of Co^{II}–Fe^{III}* pairs (with a long cell parameter). **$Na_{1.8}$** contains a majority of Co^{III}– Fe^{II} diamagnetic pairs at low temperature before irradiation. Thus, the Co–ligand bond lengthening accompanying the photo-induced electron transfer leads to strong elastic interactions between the excitable species and cooperative effects and the structural effects are evidenced by our diffraction data (Fig. 3). The associated magnetic consequences appear in the abrupt spontaneous, first-order transition, with thermal hysteresis observed by Hashimoto et al. [28].

4. Conclusion

The study of the photomagnetic properties of $C_xCo_4[Fe(CN)_6]_{(8+x)/3}\square_{(4-x)/3}$ Prussian blues reveals the complexity of the excitation process. Several parameters are implied: (a) the amount of diamagnetic pairs at low temperature before irradiation; (b) the flexibility of the inorganic network linked to the amount of $[Fe(CN)_6]$ vacancies; (c) the amount and the nature of the alkali cation.

In the present study we evidenced a discontinuity in the photomagnetic properties change with the insertion rate of alkali cations.

1. For compounds with $x < 1$, the photomagnetism is due to the presence at low temperature of isolated and diluted Co^{III}–Fe^{II} diamagnetic pairs, the number of which increases with the number of alkali cation in the structure. Those diamagnetic-pairs are locally and nearly totally transformed under irradiation into metastable Co^{II}–Fe^{III}* magnetic ones. The process occurs without crystallinity loss. The structure is flexible enough to allow the lengthening of the Co-ligand bond accompanying the photo-induced electron transfer. The process is a second-order transformation.
2. For all compounds with $x \geq 1$, a majority of Co^{III}–Fe^{II} diamagnetic pairs is present, but the photomagnetic efficiency strongly depends on the amount and on the nature of the alkali cation. For those compounds, the determining factor of photomagnetism is the flexibility of the inorganic network, which decreases when the amount of alkali cation increases, the amount of $[Fe(CN)_6]$ vacancies decreases, and the size of the alkali cation increases.
3. Our study points out that sodium derivatives are more efficient than the others and that the most efficient compound among them should be $Na_1Co_4[Fe(CN)_6]_3\square_1$. It should contain one alkali cation and one vacancy per cell. Then it should be composed of a majority of diamagnetic pairs and should contain enough $[Fe(CN)_6]$ vacancies giving a maximum flexibility to the network. The compound has already been synthesized by Hashimoto and co-workers [28] and seems effectively to be the most efficient of the whole CoFe family.

Acknowledgements

We thank Françoise Villain for X-ray absorption spectroscopy at the Co and Fe K edges, François Varret for discussions and access to SQUID magnetometer and the European Community (Grant ERBFMRXCT980181), contract TMR/TOSS (FMRX-CT98-0199) and CNRS (‘Programme Matériaux’) for financial support.

References

[1] S. Decurtins, P. Gütlich, C.P. Köhler, H. Spiering, A. Hauser, Chem. Phys. Lett. 105 (1984) 1.
[2] S. Decurtins, P. Gütlich, M.K. Hasselbach, A. Hauser, H. Spiering, Inorg. Chem. 24 (1985) 2174.
[3] C. Roux, J. Zarembowitch, B. Gallois, T. Granier, R. Claude, Inorg. Chem. 33 (1994) 2273.
[4] O. Sato, S. Hayami, Z.-Z. Gu, K. Seki, R. Nakajima, A. Fujishima, Chem. Lett. (2001) 874.
[5] P. Gütlich, Y. Garcia, T. Woïke, Coord. Chem. Rev. (2001) 839 and references therein.
[6] G. Rombaut, M. Verlest, S. Gohlen, L. Ouhab, C. Mathonière, O. Kahn, Inorg. Chem. 40 (2001) 1151.
[7] S. Ohkoshi, N. Mashida, Z.J. Zhong, K. Hashimoto, Synth. Met. 122 (2001) 523.
[8] S. Ohkoshi, K. Hashimoto, J. Am. Chem. Soc. 121 (1999) 10591.
[9] F. Varret, M. Noguès, A. Goujon, in: J. Miller, M. Drillon (Eds.), Magnetism: ‘Molecules to Materials’, Vol. 2, Wiley-VCH, Weinheim, 2000, p. 257.
[10] O. Sato, T. Iyoda, A. Fujishima, K. Hashimoto, Science 272 (1996) 704.
[11] A. Goujon, O. Roubeau, F. Varret, A. Dolbecq, A. Bleuzen, M. Verdaguer, Eur. Phys. J. B 14 (2000) 115.

[12] C. Cartier dit Moulin, F. Villain, A. Bleuzen, M.-A. Arrio, P. Sainctavit, C. Lomenech, V. Escax, F. Baudelet, E. Dartyge, J.-J. Gallet, M. Verdaguer, J. Am. Chem. Soc. 122 (2000) 6653.
[13] O. Sato, Y. Einaga, T. Iyoda, A. Fujishima, K. Hashimoto, J. Electrochem. Soc. 144 (1997) L11.
[14] O. Sato, Y. Einaga, T. Iyoda, A. Fujishima, K. Hashimoto, J. Phys. Chem. B 101 (1997) 3903.
[15] Y. Einaga, S. Ohkoshi, O. Sato, A. Fujishima, K. Hashimoto, Chem. Lett. (1998) 585.
[16] O. Sato, Y. Einaga, A. Fujishima, K. Hashimoto, Inorg. Chem. 38 (1999) 4405.
[17] D.A. Pejacovic, J.L. Manson, J.S. Miller, J. Appl. Phys. 87 (2000) 6028.
[18] D.A. Pejacovic, J.L. Manson, J.S. Miller, Phys. Rev. Lett. 85 (2000) 1994.
[19] A. Goujon, F. Varret, V. Escax, A. Bleuzen, M. Verdaguer, Polyhedron 20 (2001) 1339.
[20] A. Goujon, F. Varret, V. Escax, A. Bleuzen, M. Verdaguer, Polyhedron 20 (2001) 1347.
[21] T. Kawamoto, Y. Asai, S. Abe, Phys. Rev. B 60 (1999) 12990.
[22] M. Verdaguer, Science 272 (1996) 698.
[23] A. Bleuzen, C. Lomenech, A. Dolbecq, F. Villain, A. Goujon, O. Roubeau, M. Nogues, F. Varret, F. Baudelet, E. Dartyge, C. Giorgetti, J.-J. Gallet, C. Cartier dit Moulin, M. Verdaguer, Mol. Cryst. Liq. Cryst. 335 (1999) 965.
[24] A. Bleuzen, C. Lomenech, V. Escax, F. Villain, F. Varret, C. Cartier dit Moulin, M. Verdaguer, J. Am. Chem. Soc. 122 (2000) 6648.
[25] V. Escax, A. Bleuzen, C. Cartier dit Moulin, F. Villain, A. Goujon, F. Varret, M. Verdaguer, J. Am. Chem. Soc. 123 (2001) 12636.
[26] G. Champion, V. Escax, C. Cartier dit Moulin, A. Bleuzen, F. Villain, F. Baudelet, E. Dartyge, M. Verdaguer, J. Am. Chem. Soc. 123 (2001) 12544.
[27] V. Escax, thèse, université Pierre-et-Marie-Curie, Paris, 2002.
[28] N. Shimamoto, S. Ohkoshi, O. Sato, K. Hashimoto, Inorg. Chem. 41 (2002) 678.